shows that the wave amplitude of the most unstable mode varies strongly with height. It is possible that variation in the level of the observed cloud top contributes to the irregularity of the observed wind oscillations. A variation in the zonal wind profile or in the trapping properties of the atmosphere could also cause the wave to appear sometimes but not at other times. Our analysis of Pioneer Venus observations shows that velocity oscillations may appear for a few days, disappear, and then reappear with a phasing unrelated to the previously observed oscillation. This sort of behavior is consistent with the low Q associated with the waves in our computation.

Energy sources other than cloud feedback are possible. Instability of horizontal shear is an obvious candidate excluded by assumption from the modeling reported here. The key point is that a low-order global wave mode that appears to have the correct kinematic properties has been identified. In the absence of a forcing mechanism, it is estimated to decay with about a 20-day time scale. Cloud feedback seems to have the right magnitude to provide the forcing and also seems to pick out the correct phase velocity for the most unstable mode, but we have not excluded other possibilities for excitation.

REFERENCES AND NOTES

1. A. Seiff *et al.* [*J. Geophys. Res.* **85**, 7903 (1980)] reported the thermodynamic structure of the Venus atmosphere as measured by the NASA Pioneer Venus probes in 1979. Optical properties of the cloud tops were discussed by K. Kawabata *et al.* (*ibid.*, p. 8129).
2. The latitudinal profile of cloud-top winds varies over time, and the mid-latitude jets are sometimes almost absent. The 1974 profile was measured by S. S. Limaye and V. E. Suomi [*J. Atmos. Sci.* **38**, 1220 (1981)]; the 1979 profile by W. B. Rossow, A. D. DelGenio, S. S. Limaye, and L. D. Travis [*J. Geophys. Res.* **85**, 8107 (1980)]; and the 1982 profile by S. S. Limaye, C. Grassotti, and M. J. Kuetemeyer [*Icarus* **73**, 193 (1988)]. Profiles for 1980 and 1983 were measured by us and are presented in (*19*).
3. The vertical wind profile, based on tracking Pioneer Venus probe drifts, was found to be similar at four widely separated locations [C. C. Counselman III, S. A. Gourevitch, R. W. King, G. B. Loriot, *J. Geophys. Res.* **85**, 8026 (1980)].
4. M. J. S. Belton, G. R. Smith, D. A. Elliott, K. Klaasen, G. E. Danielson, *J. Atmos. Sci.* **33**, 1383 (1976); W. B. Rossow, A. D. DelGenio, S. S. Limaye, L. D. Travis, *J. Geophys. Res.* **85**, 8107 (1980).
5. M. J. S. Belton, G. R. Smith, G. Schubert, A. D. DelGenio, *J. Atmos. Sci.* **33**, 1394 (1976).
6. A. D. DelGenio and W. B. Rossow, *ibid.* **47**, 293 (1990).
7. A collection of articles on the Galileo flyby and the associated ground-based campaign was published in *Science* [**253**, 1516–1550 (1991)].
8. M. J. S. Belton *et al.*, *ibid.*, p. 1531.
9. See D. Crisp *et al.*, *ibid.*, p. 1538, and references therein.
10. C. Covey and G. Schubert, *J. Atmos. Sci.* **39**, 2397 (1982).
11. A convenient parameterization of the basic state wind and temperature profiles in the Venus atmosphere was introduced by R. E. Young *et al.*, *ibid.* **44**, 2628 (1987). We experimented with the sensitivity of wave modes to alterations in the basic state. The lowest modes, which turn out to be the ones of principal interest, are not highly sensitive to variations of the basic state that are consistent with observational variability or uncertainty.
12. We fitted a smooth function to the radiative time constant estimates by D. Crisp [*Icarus* **77**, 391 (1989)] for altitudes above ~60 km, and for a disturbance with vertical wavelength of ~20 km, roughly consistent with our calculated results. At altitudes less than 60 km, we followed the estimates by J. B. Pechmann and A. P. Ingersoll [*J. Atmos. Sci.* **41**, 3290 (1984)].
13. R. G. Knollenberg and D. M. Hunten [*J. Geophys. Res.* **85**, 8039 (1980)] presented data from the Pioneer Venus particle size spectrometer experiment.
14. R. G. Knollenberg *et al.* (*ibid.*, p. 8059) calculated optical depths from the data presented in (*13*). There are about 20 optical depths at visible wavelengths within a layer that is 7 km thick (this is approximately a pressure scale height). M. G. Tomasko *et al.* (*ibid.*, p. 8187) estimated cross sections in the thermal infrared to be about half of those in the visible, which places the cloud in the optically thick regime.
15. M. G. Tomasko, L. R. Doose, P. H. Smith, A. P. Odell, *ibid.*, p. 8167.
16. Cloud instabilities of this type have been studied by P. J. Gierasch, A. P. Ingersoll, and R. T. Williams [*Icarus* **19**, 473 (1973)] and by S. J. Ghan [*J. Atmos. Sci.* **46**, 2529 (1989)].
17. M. S. Longuet-Higgins [*Proc. R. Soc. London Ser. A* **262**, 511 (1968)] discussed the horizontal structure of waves on a rotating planet. We used his calculations to check our numerical procedure.
18. L. W. Esposito, *Science* **223**, 1072 (1984).
19. P. J. Schinder, P. J. Gierasch, S. S. Leroy, M. D. Smith, *J. Atmos. Sci.* **47**, 2037 (1990).
20. The phasing is chosen so that the maximum eastward perturbation in zonal velocities is in phase with the maximum northward perturbation in meridional velocities. The zonal wave amplitude is 10 m s^{-1}, and the meridional wave amplitude is 2 m s^{-1}. This phasing and amplitude are consistent with the results of our computation and with observations.

21. This work was supported by the NASA Galileo Project, the NASA Pioneer Venus Project, and the NASA Planetary Atmospheres Program. The computations were performed at the Cornell National Supercomputer Facility, which is supported by Cornell University, IBM, and the National Science Foundation. We thank M. J. S. Belton, C. Leovy, and two anonymous referees for helpful criticism.

24 December 1991; accepted 9 March 1992

Protein Solvation in Allosteric Regulation: A Water Effect on Hemoglobin

Marcio F. Colombo,* Donald C. Rau, V. Adrian Parsegian

The oxygen affinity of hemoglobin varies linearly with the chemical potential of water in the bathing medium, as seen from the osmotic effect of several neutral solutes, namely sucrose, stachyose, and two polyethyleneglycols (molecular weights of 150 and 400). The data, analyzed either by Wyman linkage equations or by Gibbs-Duhem relations, show that ~60 extra water molecules bind to hemoglobin during the transition from the fully deoxygenated tense (T) state to the fully oxygenated relaxed (R) state. This number, independent of the nature of the solute, agrees with the difference in water-accessible surface areas previously computed for the two conformations. The work of solvation in allosteric regulation can no longer go unrecognized.

The regulation of protein or enzymatic activity is often accomplished through the control of equilibrium among allosteric conformations. Differences in binding affinities of small effector molecules to specific regulatory sites among these conformations modulate this equilibrium. For hemoglobin (Hb), the prototypic allosteric protein, equilibrium between R and T conformations, and consequently its oxygen (O_2) affinity, is modulated by the binding of several small molecules and ions, such as H^+, CO_2, phosphates, and Cl^-. The structures of the two limiting conformations show that several direct contacts between subunits are broken and exposed to solvent during the transition from deoxy T state to the fully oxygenated R state (*1*). This change in structure implies a difference in hydration or water binding between the two conformations. However, the energetic consequences of solvation regulating protein activity are usually neglected.

Such water sensitivity can, in fact, be probed through the dependence of O_2 affinity on water activity or, equivalently, osmotic pressure. This "osmotic stress" method (*2*) has been used to measure intermolecular forces (*3*), to map the thermodynamics of Hb S assembly (*4*), to measure the change in aqueous volume of a large, voltage-gated ionic channel (*5*), and to modify the electron transfer reaction in cytochrome C oxidase (*6*).

The linkage between O_2 uptake and ligand concentration is most often analyzed by relations developed by Wyman (*7*). The

M. F. Colombo and D. C. Rau, Laboratory of Biochemistry and Metabolism, National Institute of Diabetes and Digestive and Kidney Diseases, National Institutes of Health, Bethesda, MD 20892.
V. A. Parsegian, Physical Sciences Laboratory, Division of Computer Research and Technology and Laboratory of Biochemistry and Metabolism, National Institute of Diabetes and Digestive and Kidney Diseases, National Institutes of Health, Bethesda, MD 20892.

*On leave from Departamento de Física, IBILCE-UNESP, São José do Rio Prêto, São Paulo, Brazil.

common usage of these equations, however, implicitly assumes that the activity of one solution component is varied while all others are held constant. It is, of course, not possible to change the concentration of a single solute without also affecting the activity of water. Thus, changes in the affinity of Hb for O_2 with the concentration of small solutes reflect the energetics not only of removing bound solutes from the bulk solution, but also of removing hydration water. An important criterion for discriminating between direct solute binding and osmotic effects is the sensitivity to the chemical nature of the solute. A strictly osmotic effect would not depend on solute identity. A dependence of Hb O_2 affinity on the concentration of several small, neutral solutes has been observed previously (*8*), but it has not been specifically analyzed for the indirect effect on water activity.

In this report, we explicitly consider the linkage between water activity and O_2 affinity. We infer from the data that ~60 extra water molecules are bound in the deoxy-to-oxy transition. These water molecules act thermodynamically as allosteric ligands and provide an essential energetic contribution to the functional regulation of Hb.

The ligand binding properties of Hb can be well described by the Gibbs-Duhem relation. At constant temperature and hydrostatic pressure, we have for an Hb solution with an average number of O_2 (n_{O_2}), water (n_w), and other solute molecules (n_L) associated per mole of protein:

$$d\mu_{Hb} = -n_{O_2}d\mu_{O_2} - n_w d\mu_w - \Sigma n_L d\mu_L \quad (1)$$

where μ_{Hb}, μ_{O_2}, μ_w, and μ_L are the chemical potentials of protein, oxygen, water, and other solutes in solution, respectively (*9*). Equivalently, solution components can be considered as surface-active compounds regulating the free energy of a protein surface (*10*).

Several Maxwell relations can be written based on Eq. 1, relating changes in $\{n_i\}$ to changes in $\{\mu_i\}$. If there is no change in binding of solute with oxygenation, that is, $(\partial n_L/d\mu_{O_2})_{\mu_w} = 0$, then a particular Maxwell relation connecting changes in the number of associated waters n_w and oxygens n_{O_2} with changes in O_2 and water chemical potentials is:

$$(\partial n_w/d\mu_{O_2})_{\mu w, \ldots} = (\partial n_{O_2}/\partial \mu_w)_{\mu_{O_2}, \ldots} \quad (2)$$

This basic linkage relation allows one to measure changes in water binding, or protein hydration, due to molecular events triggered by changes in O_2 binding. For a simple osmotic stress effect, the chemical identity of the solute is unimportant and only the osmolality matters.

The term $(\partial n_{O_2}/\partial \mu_w)_{\mu O_2}$ is the experimentally measurable change in O_2 binding at constant O_2 activity with a change in water activity. Integrating this quantity over all O_2 pressures gives the total change of water, $\Delta n_w = (n_w^{oxy} - n_w^{deoxy})$, associated with Hb in the transit from the fully deoxygenated to the fully oxygenated state, that is,

$$\Delta n_w = \int (\partial n_{O_2}/\partial \mu_w)_{\mu_{O_2}} d\mu_{O_2} \quad (3)$$

Several reciprocal differential relations like Eq. 2 can be derived to describe the interplay of O_2 activity and binding with ligand activity and binding. The linkage equations presented by Wyman (*7*) have in particular been widely applied to Hb oxygenation thermodynamics. A general relation for the coupling of μ_{O_2} and n_{O_2} with the binding of any solution component n_x and its chemical potential, μ_X, is

$$(\partial \mu_{O_2}/\partial \mu_X)_{n_{O_2}, \ldots} = (\partial n_X/\partial n_{O_2})_{\mu_X, \ldots} \quad (4)$$

Wyman (*7*) introduced a median ligand activity, p_m, to describe the full transition from deoxy to oxy form. For $\Delta n_{O_2} = 4$, Eq. 4 can then be expressed as

$$d\log(p_m)/d\log(a_X) = -\Delta n_X/4 \quad (5)$$

To good approximation p_m is p_{50}, the oxygen partial pressure at half saturation of Hb. The slope of $\log(p_{50})$ versus $\log(a_X)$ gives Δn_X, the difference between the number of X associated with oxy and deoxy Hb.

Table 1. Sensitivity of $\log(p_{50}/p_{50}^{\circ})$ on osmotic stress for Hb determined by fitting Eq. 5 to the experimental data.

Solute	$d\log[p_{50}/p_{50}^{\circ}]/d\Pi \times 10^3$ (atm^{-1})	Standard deviation $\times 10^3$ (atm^{-1})
Sucrose	4.74	0.25
Stachyose	4.42	0.51
PEG-150	4.91	0.38
PEG-400	4.78	0.54
Mean value	4.71	0.13

When X refers specifically to water, Δn_X is equivalent to the Δn_w of Eq. 3.

The presence of neutral solutes in the Hb solution changes its O_2 affinity. In Fig. 1, the fraction of O_2 saturation of Hb, $\bar{n}_{O_2}$ versus $\log(p_{O_2})$, is shown for different sucrose concentrations. Similar experiments with other solutes, PEG-150, PEG-400, and stachyose, display the same behavior, that is, a decrease in O_2 affinity with the increase of neutral solute concentration. Calculated Hill coefficients are independent of solute concentrations over the ranges measured.

For consideration below, we further plot the data in two different ways. In Fig. 2, the

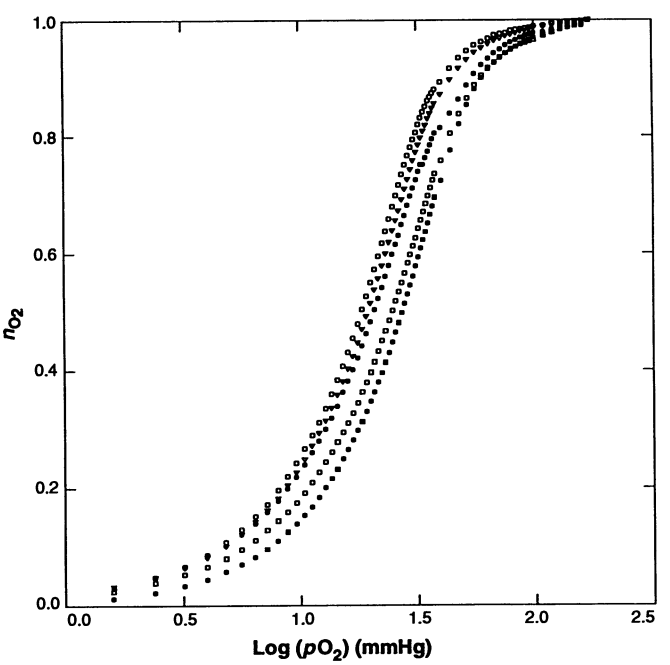

Fig. 1. Influence of osmotic pressures (Π) from different sucrose concentrations on Hb oxygenation: 1.8 (○), 7.7 (▽), 17.3 (0), 34.4 (□), and 43 atm (■). Hemoglobin samples (*21*) were buffered with 0.1 M NaCl/0.05 M tris, pH 6.93, at 37°C. Sucrose (Ultra pure, BRL), stachyose (Sigma), triethylene glycol (molecular weight 150), and polyethylene glycol (PEG), average molecular weight 400 (both from Fluka Chemika), were used without further purification. Hemoglobin concentration and met-Hb content were measured spectrophotometrically using published extinction coefficients (*9*). The osmolalities of the various solutions were measured with a Wescor 5100 C Vapor Pressure Osmometer. Hemoglobin O_2 binding curves were measured at 37°C and a protein concentration of about 1 mM tetramer [a concentration high enough to obviate problems of dimerization (*13*)] using a Hemo-O-Scan Oxygen Dissociation Analyser (SLM-Aminco, Silver Spring, Maryland). The samples were typically deoxygenated by 5.6% of CO_2 in nitrogen and reoxygenated with 25% O_2, 5.6% CO_2 in nitrogen. The same sensitivities of p_{50} to osmotic pressure were obtained using gasses with no CO_2. Concern over any small leaks was allayed by the observation of identical results with the unmodified Hemo-O-Scan and a modification sealing with silicone grease and enclosure in a plastic bag. Manual operation of the gas valves to give a very slow rate of oxygenation showed that the measured curves are equilibrium curves. The original curves were digitized in a Nunomics 2200 digitizer (Jandel Scientific) for further analysis. To within the accuracy allowed by the Hemo-O-Scan, the oxygen loading of myoglobin showed no sensitivity to osmotic stress.

log of the ratio of O_2 partial pressures at half saturation with and without added solute, $\log[p_{50}/p^{\circ}_{50}]$, is shown versus osmotic pressure Π for the four neutral solutes. In Fig. 3, we plot the same data as $\log[p_{50}/p^{\circ}_{50}]$ versus log[X] where [X] is the molar solute concentration.

These data show that 50 to 70 solute-excluding water molecules become part of the Hb tetramer in its transition from the deoxy to oxy form. We consider several possibilities for the action of the neutral solutes and use linkage relations to convert the osmotic sensitivity of Hb into a measure of protein hydration change.

Within the solute concentration ranges used, no change in the visible spectrum of the protein is observed, indicating that neither direct competition between solute and O_2 nor the formation of hemi- or hemochrome derivatives, which occurs at higher solute concentration (*11*) and lower water activity (*12*), can explain the results shown in Fig. 1. Neither can changes in dimer-tetramer equilibrium. At 1 mM tetramer concentration, dimer concentration is extremely low (*13*). Even at much lower concentrations, the tetramer-dimer equilibrium appears not to change with added sucrose (*14*).

The change in O_2 affinity reflects either direct interaction between the neutral solutes and the protein or changes in solution properties. One may think of different amounts of solute bound to each of the two forms of Hb or one may view the action of solute primarily through its effect on water activity and changes in protein hydration for the different conformational states.

To examine the possibility of direct solute interaction with the protein, we plotted, in Fig. 3, $\log[p_{50}/p^{\circ}_{50}]$ versus log[X], where [X] is the molar solute concentration. This procedure is typical for analyzing data assuming only a change in direct solute binding. Unless there is strong cooperativity or very weak solute binding, the dependence of p_{50} on log[X] should be linear. It is not.

Still, if we force a linear fit to the data and apply the Wyman linkage relation, Eq. 5, then an approximate difference in average number of bound solutes in the full oxy and full deoxy of $\Delta n_X = -1.0 \pm 0.3$ is found for all four solutes.

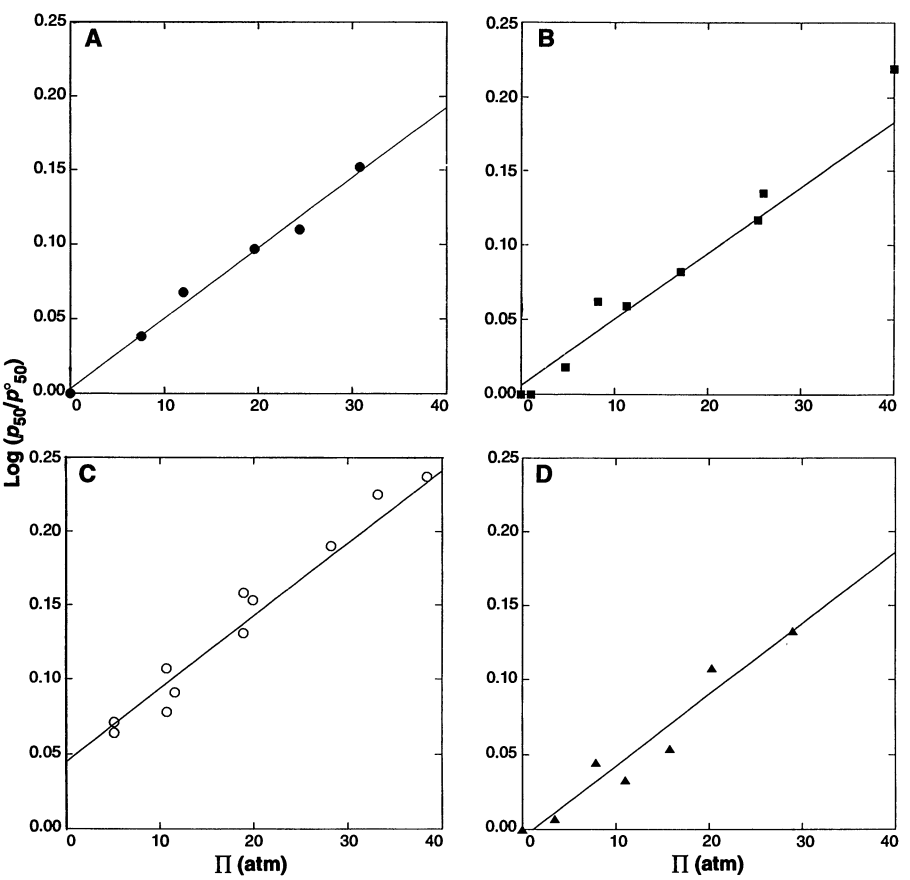

Fig. 2. The relative shift in p_{O_2} at half saturation, $\log(p_{50}/p^{\circ}_{50})$, with increasing solute concentration is shown as dependent on solution osmotic pressure (Π) due to the action of different solutes: (**A**) sucrose, (**B**) stachyose, (**C**) PEG-150, and (**D**) PEG-400. The solid lines are the best nonlinear fits of the data with parameters shown in Table 1. The PEG-150 data does not extrapolate to p°_{50} at $\Pi = 0$. There is a shift in oxygen affinity that occurs at very low PEG-150 concentration. We do not know the origin of this. The slope of this plot, $d\log[p_{50}/p^{\circ}_{50}]/d\Pi$, however, is unaffected within the experimental error.

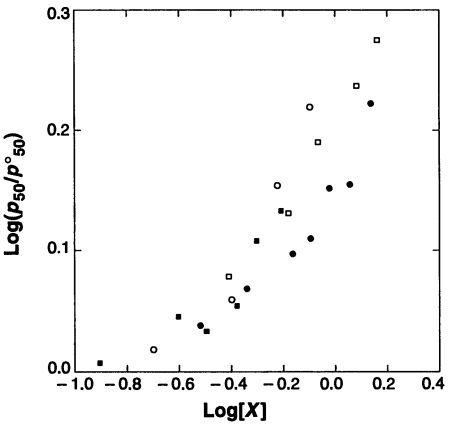

Fig. 3. The relative shift $\log(p_{50}/p^{\circ}_{50})$ with increasing solute concentration is shown as dependent on solute activity, log(*X*), for sucrose (○), stachyose (●), PEG-150 (□), and PEG-400 (■).

Superficially, this last result obtained assuming only solute binding could be considered quite reasonable. However, a closer look at the data and at the measured interaction energies between sugars or PEGs and protein surfaces makes this interpretation improbable. The linkage plots in Fig. 3 for all four solutes closely superimpose. Unlike the expected common water linkage curve in Fig. 2 for all solutes (to be considered further below), the common plot here means that binding characteristics are independent of the chemical nature of the solute. Not only must there be binding of the sugars and the PEGs, but also the binding characteristics, that is the number of sites, and binding constants, must be closely and improbably similar for polyol sugars and for polyether PEGs despite their very different chemical properties.

The indirect action of solute through water activity is tested by plotting the shift

Table 2. Change in the number of water molecules per tetramer of Hb from fully deoxy to fully oxy form as determined in different solvents.

Solute	$\Delta n_w \pm$ standard deviation determined from Eq. 5*	Δn_w determined by integrating Eq. (3)†
Sucrose	60 ± 3.2	76
Stachyose	56 ± 6.4	68
PEG-150	62 ± 4.8	60
PEG-400	60 ± 6.8	57
Mean value ± standard deviation	60 ± 2	65 ± 4

*Wyman equation. †Integration of Gibbs-Duhem equation.

in $\log[p_{50}/p_{50}^{\circ}]$ versus Π for all four solutes (Fig. 2). Here the plots are clearly linear, indicating a linkage to a well-defined and constant difference in number of bound waters. Slopes are the same for all four solutes (Table 1).

Differential hydration of the protein with no direct solute binding is sufficient to describe the suppression of O_2 uptake. The effect of the solute on O_2 affinity is indirect, acting through its effect on water activity.

From Eq. 5, the slope of the common line in Fig. 2 gives the difference in the number of bound water molecules between the R and T conformations, that is, the total number of waters acting as allosteric effectors. Values of $\Delta n_w = n_w^{oxy} - n_w^{deoxy}$ with standard deviations, from the Wyman linkage relation applied to the data for each solute, are summarized in Table 2. Averaging the Δn_w over the different solutes, we find $\Delta n_w = +60 \pm 2$ waters.

One finds essentially the same number of binding water molecules using Eq. 3 derived from the Gibbs-Duhem equation. The numerical evaluation of the partial derivative $(\partial \bar{n}_{O_2}/\partial \mu_w)|\mu_{O_2}$ from the oxygenation data is straightforward. The dependence of $\bar{n}_{O_2}$ on sucrose osmotic pressure at five p_{O_2} values is shown in Fig. 4. Interestingly, these plots are all well described by a linear correlation between O_2 binding and water chemical potential.

The number of water molecules linked with full oxygenation is obtained by integrating this osmotic sensitivity of Hb O_2 binding at fixed O_2 activity over the entire range of O_2 chemical potentials. The dependence of $(\partial n_{O_2}/\partial \Pi)|\mu_{O_2}$ on $\log(p_{O_2})$ is shown in Fig. 5. The area defined under this curve gives Δn_w. The results of integration for each of the four solutes are summarized in Table 2. The average number of extra water molecules bound in the deoxy to full oxy transition calculated by this method is 65 ± 4.

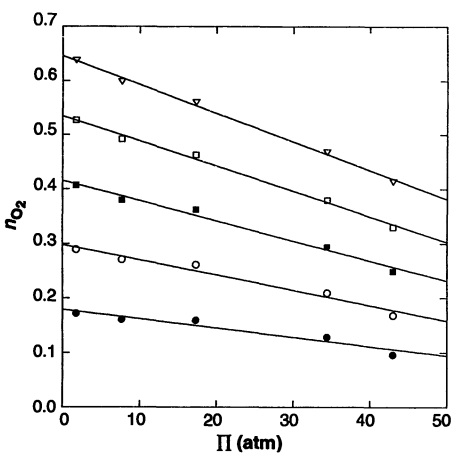

Fig. 4. The fraction of O_2 saturation, n_{O_2}, is shown as dependent on sucrose osmotic pressure shown for five p_{O_2} values: 7.2 (○), 11.2 (●), 15.2 (■), 19.2 (□), and 23.2 mmHg (▽). The slopes of the linear fits give $(dn_{O_2}/d\Pi)|\mu_{O_2}$.

This value is somewhat larger (~10%) than that calculated with the Wyman equation from the sensitivity of p_{50} on osmotic pressure. The integration method, however, is more sensitive to small systematic errors in estimating Hb O_2 saturation and O_2 activities than the p_{50} method. The difference is probably not experimentally significant. There is also about the same difference in average Δn_w between the sugars and PEGs; again, the difference is comparatively small. In general, values of Δn_w estimated by the two methods agree quite well. The binding of some 50 to 70 extra water molecules is linked to the transition.

Arakawa and Timasheff (*15*) have directly measured the thermodynamics of sugar-protein and PEG-protein interactions for several different proteins with results pertinent to our observations. Sugars and PEGs are preferentially excluded from protein surfaces. In the range of sucrose concentrations examined here, the unfavorable interaction energies between sucrose and protein surfaces appear predominantly osmotic, that is, linearly dependent on solute concentration or water chemical potential, not on solute chemical potential. Solute exclusion energies can be correlated with increased protein stability and decreased solubility, states that minimize solute exposed surface area.

Arakawa and Timasheff (*15*) have also shown that preferential exclusion interactions of several sugars are approximately linearly dependent on accessible protein surface area. Analyzing these data as an osmotic stress results in an estimated one water molecule per 7 to 10 Å^2 protein surface area that excludes sugars. Unless the extra surface exposed in the T → R transition has a greatly different character from that of most other protein surfaces, one should expect a similar exclusion/area correlation for Hb.

Several calculations of the difference in accessible surface areas (ASA) between the deoxy T and oxy R of Hb have been reported (*16*) showing that the ligated oxy protein exposes from 500 to 800 Å^2 more surface to the solvent than the unligated deoxy form. The rotation of the $\alpha_1\beta_1$ dimer relative to the $\alpha_2\beta_2$ alone exposes 700 Å^2 (*16*). The range of surface areas reported results from different estimates for the changes in $\alpha_1\alpha_2$ contacts. There is also considerable disagreement about the change in ASA along the highly flexible $\beta_1\beta_2$ interface. Considering only the more firmly established changes on $\alpha_1\alpha_2$ and $\alpha_1\beta_1/\alpha_2\beta_2$ interfaces, and that one water molecule can cover about 9 to 10 Å^2 of a surface, one finds that 55 to 90 water

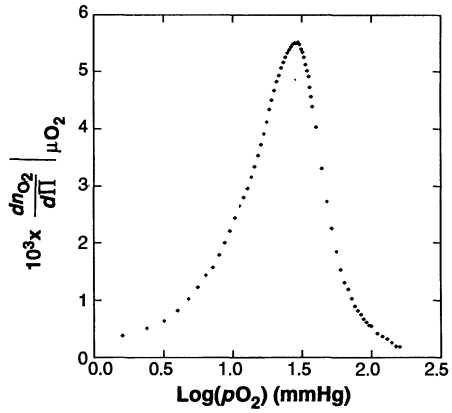

Fig. 5. The dependence of $(dn_{O_2}/d\Pi)|\mu_{O_2}$ on log of partial pressure is shown. The area defined under this curve gives (1/4) $\Delta n_w \bar{v}_w/2.303\,RT$ (R, gas constant; T, temperature). The factor 4 accounts for the 4 oxygen bound per mole of Hb tetramer at full saturation.

molecules are necessary to hydrate the extra surface on oxy-Hb. The 60 water molecules we infer agree well with the estimated accessible surface area change.

There are two basic contributions of these 60 water molecules to the energy difference between T and R states. The energy from transferring these waters from bulk solution to the new protein surface of the R state is the osmotic work we measure. There is also the very large energy associated with the interaction energies of these water molecules with the protein surface. Transfer energies alone can be significant. Compared to pure water, the osmotic work for binding these 60 water molecules to the R state is about 0.2 kcal/mol Hb in a physiological medium (~0.28 osmol or some 6 atm). This 0.2 kcal/mol is an increase in allosteric energy of interaction due to the natural osmolyte concentration in the red cell.

Water formally acts as any allosteric ligand, but, unlike any other ligand, water is the only one that is always active. It is doubtful that the R state would even exist without the stabilization promoted by hydration of the extra surface. We are forced to recognize the importance of solvation in protein regulation.

From here we are led to think in several new directions. Recent measurements of forces acting between many biopolymers (*3*) show the importance of water structuring to macromolecular interactions. Can the enormous energies derived from these measured hydration forces now be connected with the solvation energies of protein surfaces that act in allostery? These hydration energies, perhaps acting to spread solvent-exposed surfaces, can be an excellent candidate for the delocalized energies postulated by Hopfield (*17*) to explain changes

in O_2 affinity without large changes in structure (*18*).

It is clear that thermodynamically/energetically significant waters of solvation are not equivalent to the much more tightly bound waters that can be seen by x-ray or neutron diffraction although these "visible" waters can be among those seen thermodynamically.

Intermediate states have been recently postulated for the R-T transition in Hb (*19*). Can the total 60 water molecules we measure be assigned to specific molecular events and the osmotic stress method able to recognize structural intermediates?

The action of other ligands must be reexamined to recognize their concomitant influence on water activity. Here we have only considered the two extreme cases: that there is only direct solute binding ($\Delta n_w = 0$) or only an indirect effect of solute on water binding ($\Delta n_X = 0$). Considering only water binding gives the best agreement between thermodynamic expectations and the experimental data for these solutes. A more general treatment for solutes that do bind as well as change water properties would include both direct and indirect actions. We will present elsewhere work reanalyzing the effect of Cl^- on Hb in terms of both water and ion binding (*20*).

Solvent influence on regulation of Hb-based artificial blood preparations can differ from that of the highly controlled intracellular milieu of erythrocytes. Water activity must be a consideration in system design.

Finally, one can see a unity between allosteric proteins and the several transport proteins (*5*, *6*) where different functional states have measurably different levels of hydration.

REFERENCES AND NOTES

1. J. Baldwin and C. Chothia, *J. Mol. Biol.* **129**, 175 (1979).
2. V. A. Parsegian, R. P. Rand, D. C. Rau, *Methods Enzymol.* **127**, 400 (1986).
3. R. Podgornik, D. C. Rau, V. A. Parsegian, *Macromolecules* **22**, 1780 (1989); D. C. Rau and V. A. Parsegian, *Science* **249**, 1278 (1990); R. P. Rand and V. A. Parsegian, *Biochem. Biophys. Acta* **988**, 351 (1989).
4. M. S. Prouty, A. N. Schechter, V. A. Parsegian, *J. Mol. Biol.* **184**, 517 (1985).
5. J. Zimmerberg and V. A. Parsegian, *Nature* **323**, 36 (1986); J. Zimmerberg, F. Bezanilla, V. A. Parsegian, *Biophys. J.* **57**, 1049 (1990).
6. J. A. Kornblatt and G. H. B. Hoa, *Biochemistry* **29**, 9370 (1990).
7. J. Wyman, *Adv. Protein Chem.* **19**, 223 (1964); _____ and S. J. Gill, *Binding and Linkage, Functional Chemistry of Biological Macromolecules* (University Science, Mill Valley, CA, 1990).
8. R. N. Haire and B. E. Hedlund, *Biochemistry* **22**, 327 (1983); L. Cordone, A. Cupane, S. L. Fornili, *Biopolymers* **22**, 1677 (1983).
9. E. Di Cera, *Biophys. Chem.* **37**, 147 (1990).
10. M. Blank, *Colloids Surf.* **1**, 139 (1980).
11. A. C. I. Anusiem, J. G. Beetlestone, J. B. Kushimo, A. A. Oshodi, *Arch. Biochem. Biophys.* **175**, 138 (1976).
12. M. F. Colombo and R. Sanches, *Biophys. Chem.* **36**, 33 (1990).
13. F. C. Mills, M. L. Johnson, G. K. Ackers, *Biochemistry* **15**, 5350 (1976).
14. A. Brancaccio, A. Bellelli, M. Brunori, personal communication.
15. T. Arakawa and S. N. Timasheff, *Biochemistry* **21** 6536 (1982).
16. C. Chothia, S. Wodak, J. Janin, *Proc. Natl. Acad. Sci. U.S.A.* **73**, 3793 (1976); J. Janin and S. J. Wodak, *Biopolymers* **24**, 509 (1985); A. M. Lesk, J. Janin, S. Wodak, C. Chothia, *J. Mol. Biol.* **183**, 267 (1985).
17. J. J. Hopfield, *J. Mol. Biol.* **77**, 207 (1973).
18. M. Perutz, *Mechanism of Cooperativity and Allosteric Regulation in Proteins* (Cambridge Univ. Press, Cambridge, 1990).
19. G. K. Ackers, *Biophys. Chem.* **37**, 371 (1990).
20. M. F. Colombo *et al.*, in preparation.
21. Human red cells were washed three times in isotonic salt solutions and lysed with distilled water. Debris was removed by 15,000-rpm centrifugation at 4°C for 1 hour with a Sorvall RC-5B Centrifuge. Protein solutions were eluted over a PD10 Sephadex G-25M column (Pharmacia) in 0.1 M NaCl, 0.05 M tris, pH 7.5, and Hb was concentrated by centrifugation with a Centricon-30 microconcentrator (Amicon). All pH measurements were done with a Radiometer pH meter 26. The preparation procedure was slightly modified from that described by A. Riggs [*Methods Enzymol.* **76**, 5 (1981)].

22. We are deeply grateful for characteristically perceptive and informative comments from G. Ackers, J. Bonaventura, C. Bonaventura, M. Brunori, W. Eaton, F. Ferrone, P. Rand, and G. Weber. M.F.C. is grateful to the CNPQ of Brazil for partial financial support and to the NIH for the award of a Visiting Scientist.

2 December 1991; accepted 10 March 1992

An Origin of DNA Replication and a Transcription Silencer Require a Common Element

David H. Rivier and Jasper Rine

A eukaryotic chromosomal origin of replication was identified in the yeast *Saccharomyces cerevisiae*. By several criteria, including map position, deletion analysis, and a synthetic form of saturation mutagenesis, the origin co-localized with the *HMR-E* silencer, which is a DNA element that represses transcription of the adjacent genes. A specific site within the silencer was required for both initiation of chromosomal replication and for repression of transcription. This analysis directly demonstrates that initiation of eukaryotic chromosomal replication is dependent on specific sequence elements and that a particular element can act in both initiation of chromosomal replication and regulation of transcription.

DNA replication is perhaps the most precisely regulated protein–nucleic acid interaction in biology; each base pair in the genome is replicated once and only once every cell division. Much of this regulation of replication may occur at chromosomal origins, the sites at which replication initiates. Specifically, in eukaryotes many origins must initiate to replicate the entire genome yet reinitiation at all origins must be prevented until the next cell cycle. Eukaryotic initiation of replication is regulated in at least two additional ways. Initiation is regulated during development of multicellular organisms; fewer origins initiate late in development than early in development. Initiation is also regulated temporally during S phase; different chromosomal origins or clusters of origins initiate replication at distinct times during S phase (*1*, *2*). Little is known about the molecular mechanisms that control initiation of eukaryotic DNA replication largely because chromosomal origins are ill-defined. Although a few chromosomal origins have been mapped to within a few hundred to a few thousand base pairs, no specific sequence element has been shown to be required for the initiation of chromosomal replication (*3*–*5*).

Division of Genetics, 401 Barker Hall, Department of Molecular and Cell Biology, University of California, Berkeley, CA 94720.

We have focused on two aspects of DNA replication; namely, the identification of sequences required for chromosomal initiation and the possible relation between DNA replication and repression of transcription. Two lines of evidence demonstrate that DNA replication and transcription can share regulatory mechanisms. First, initiation of viral replication often depends on sequence elements and proteins that also activate transcription (*6*). Thus, eukaryotic DNA replication and transcription apparently can share common activation mechanisms. Second, activation of transcription of the late genes in bacteriophage T4 and adenovirus is dependent on replication of the phage or virus. Thus, the process of replication itself can activate transcription (*7*).

The mating-type genes of *S. cerevisiae* provide a context in which to study the possible relation between DNA replication and repression of transcription. The mating-type genes reside at three loci, *MAT*, *HML*, and *HMR*. At *MAT* (the mating-type locus) the genes are transcribed and, as a result, govern cell type. Cells carrying the *MAT***a** allele have the **a** phenotype and cells carrying the *MAT*α allele have the α phenotype (*8*). In contrast to the genes at *MAT*, the mating-type genes at *HML* and *HMR* are repressed and do not contribute to